Physics – Uspekhi **53** (8) 843 – 858 (2010)

CONFERENCES AND SYMPOSIA

PACS numbers: 01.10.Fv, **01.60.+q**, **01.65.+g**, 03.75.Hh, 67.30.er, 75.30.Ds, **75.40.–s**, **75.45.+j**, 75.50.Ee, **75.50.–y**, **76.60.–k**, **75.70.–i**

90th anniversary of the birth of A S Borovik-Romanov (Scientific session of the Physical Sciences Division of the Russian Academy of Sciences, 24 March 2010)

DOI: 10.3367/UFNe.0180.201008j.0879

The scientific session of the Physical Sciences Division of the Russian Academy of Sciences (RAS) took place on 24 March 2010 in the Conference Hall of the P L Kapitza Institute for Physical Problems, RAS.

The following reports were put on the session agenda posted on the website www.gpad.ac.ru of the Physical Sciences Division, RAS:

1. **Andreev A F** (P L Kapitza Institute for Physical Problems, RAS) "Opening address";
2. **Smirnov A I, Svistov L E, Prozorova L A** (P L Kapitza Institute for Physical Problems, RAS), **Petrenko O A** (University of Warwick, UK), **Hagiwara M** (Osaka University, Japan) "Quasi-two-dimensional antiferromagnet on a triangular lattice";
3. **Bunkov Yu M** (Institut Néel, Grenoble, France) "Bose–Einstein condensation of magnons in superfluid ^{3}He";
4. **Demokritov S O** (The University of Münster, Germany) "Kinetics and Bose–Einstein condensation of magnons at room temperature."

The articles written on the basis of these reports are published below.

PACS numbers: **01.60.+q**, **01.65.+g**, **75.50.–y**
DOI: 10.3367/UFNe.0180.201008k.0879

Opening address

A F Andreev

We are delighted to have here with us these visiting participants, so pleasant and so close to us in many ways. It is the 90th anniversary of the birth of one of our most prominent physicists — Andrei Stanislavovich Borovik-Romanov. His life story was dazzling and extraordinary, both in human and in scientific terms, and it was also very dramatic. A life full of complications.

A S Borovik-Romanov was born in 1920; he was a student when the Great Patriotic war started, and he volunteered to go to the front, to the home guard troops. Very soon he was a prisoner of war (POW). He had to go through a great deal, but as Andrei Stanislavovich used to say, he was a 'lucky devil'. When he was released from captivity in Germany — by Russian soldiers — he again became a soldier in the Soviet army. This saved his life because he came back home, not as a released former POW, but as a soldier on active duty. He told me that after release from captivity, an NKVD officer told him: "You were twice lucky: the Germans did not shoot you, and now our guys have not shot you, either." And A S (abbreviated Andrei Stanislavovich) was indeed convinced that he was very lucky in his life, that he did draw a lucky ticket. Andrei Stanislavovich was, in fact, immensely optimistic. The year he demobilized, he resumed his university studies and graduated successfully.

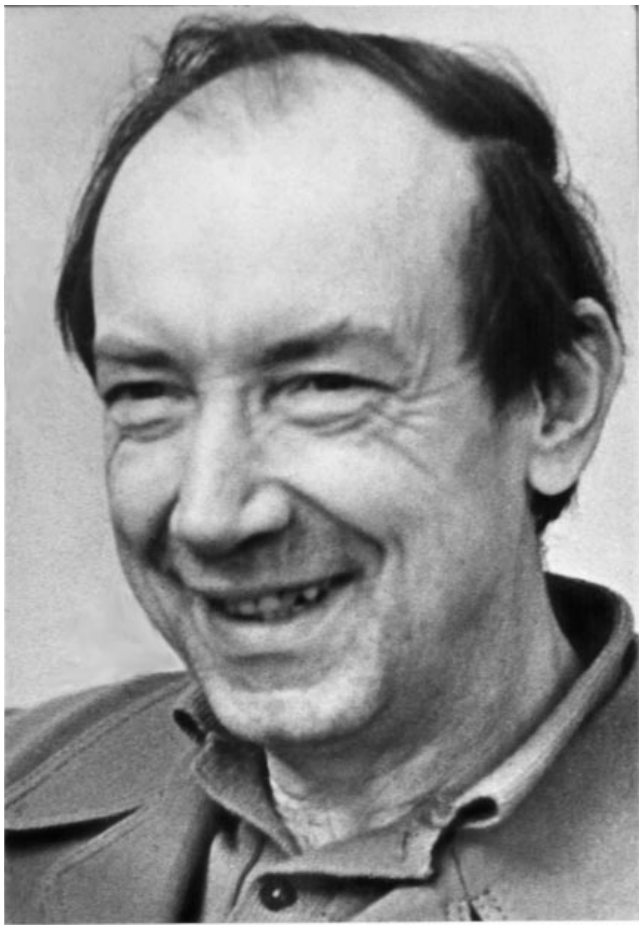

Andrei Stanislavovich Borovik-Romanov
(18.03.1920 – 31.07.1997)

Uspekhi Fizicheskikh Nauk **180** (8) 879 – 894 (2010)
DOI: 10.3367/UFNr.0180.201008j.0879
Translated by V I Kisin, S N Gorin, S O Demokritov;
edited by A Radzig

A F Andreev P L Kapitza Institute for Physical Problems,
Russian Academy of Sciences, Russian Federation
E-mail: andreev@kapiza.ras.ru

Uspekhi Fizicheskikh Nauk **180** (8) 879 – 880 (2010)
DOI: 10.3367/UFNr.0180.201008k.0879
Translated by V I Kisin; edited by A Radzig

A S Borovik-Romanov started working under the guidance of Petr Georgievich Strelkov, and soon grew to be one of the leaders among researchers in the physics of magnetic phenomena. For many years the 'official' head of the 'magnetic diaspora' here was Sergei Vasil'evich Vonsovskii, but after him Andrei Stanislavovich undoubtedly became the leader in researching magnetic phenomena.

A S first gained fame when, together with M P Orlova, he discovered weak ferromagnetism in antiferromagnets. In principle, this phenomenon had already been observed, but at that time it was assumed that it was caused by the presence of uncontrolled impurities producing incomplete compensation of the magnetic moments of two sublattices, and this resulted in a nonzero ferromagnetic moment. What A S and M P Orlova achieved was a demonstration that this phenomenon had no connection to impurities and reflected, so to speak, the nature of things.

Here again, Andrei Stanislavovich was immensely lucky — a close creative contact appeared in the person of theorist Igor Ekhiel'evich Dzyaloshinskii who also worked at our institute (IPP RAS). This collaboration generated numerous very interesting results, both theoretical and experimental. Petr Leonidovich Kapitza always pointed to it as an example of the fruitful cooperation of theory and experiment. The most important result born of it was the prediction and discovery of piezomagnetism. Many books advanced an opinion at the time that piezomagnetism was impossible because strain does not change in response to a reversal of the sign of time, while it reverses the sign of the magnetic moment. This is not true, however, if one is dealing with a state not invariant under time reversal, and any antiferromagnetic state belongs to this class. That was it: Andrei Stanislavovich discovered piezomagnetism in antiferromagnets.

Many outstanding results followed, obtained in collaboration with his students — Lyudmila Andreevna Prozorova, Natalya Mikhailovna Kreinis, and many others, for instance, Aleksandr Ivanovich Smirnov. On the whole, a fairly numerous group of brilliant people working on magnetism grew up in our institute, and they continue working on it.

Now, of course, magnetism is a far cry from what it was in the time of Borovik-Romanov — a great deal of water has flowed under the bridge — but his scientific school continues to occupy a very high level on a global scale, and what it does is precisely modern magnetism. I remember very well Andrei Stanislavovich's reaction to the discovery of the superfluidity of helium-3. That was in 1972. He was very much impressed by this discovery, especially after he realized that, in terms of magnetism, superfluid helium-3 constitutes antiferromagnet. A S then formulated the task of researching superfluid helium-3 precisely as an antiferromagnet. It is worth emphasizing at this point that even as we speak there is still not a single group within the confines of the former Warsaw Pact block which has successfully worked with superfluid helium-3. Note that Borovik-Romanov launched this research in the mid-1980s. He had built up a very creative team of young researchers: Yu M Bunkov, V V Dmitriev, Yu M Mukharskii, D A Sergatskov. Also in this team was Anita de Waard from The Netherlands and other visiting scientists. They succeeded in building a facility which is still unique and capable of achieving temperatures down to a tenth of a millikelvin.

Of high importance was Borovik-Romanov's foresight that the especially interesting features of superfluid helium-3 are not those which made superfluid helium-4 exciting (i.e., superfluidity), but precisely its magnetic properties. As a result, Andrei Stanislavovich's team discovered a novel phenomenon now known as magnetic superfluidity. A theorist also working at our institute, Igor Akindinovich Fomin, played a significant role in the discovery of this phenomenon, as well. The authors called it "homogeneously precessing domain." Nowadays, it is more fashionable to talk about Bose condensates. In these terms, this is a nonstationary Bose condensate, such that the system is in a state of coherent precession in time, while being homogeneous in space.

Andrei Stanislavovich simply loved traveling. I remember how A S and his wife at a Conference in Odessa were carefully studying the map of Odessa's environs and were enthusiastically tracing walks for independent excursions. For A S this passion proved fatal. His wish to attend the International Conference on Magnetism in Australia in July 1997 overpowered the resistance of his doctors, who were adamant that this long flight would be critically dangerous for Andrei Stanislavovich's health. However, A S insisted that he should go; alas, it was his last trip... .

A S's death was totally unexpected for everyone around him: his thoughts were about his beloved science, and he was full of plans and new ideas; alas, it was his colleagues and disciples who had to implement these plans — without Andrei Stanislavovich. The science that A S was doing continues to unfold, both at IPP RAS and in many other laboratories in various countries, as will be discussed today in subsequent research reports during this session.

PACS numbers: **75.40.–s**, 75.50.Ee, **75.70.–i**
DOI: 10.3367/UFNe.0180.2010081.0880

Triangular lattice antiferromagnet $RbFe(MoO_4)_2$

A I Smirnov, L E Svistov, L A Prozorova, O A Petrenko, M Hagiwara

The investigation of the magnetic ordering of spins on a two-dimensional triangular lattice led to the discovery of unordinary phase transitions caused by the frustration of the antiferromagnetic exchange interaction and by the effect of fluctuations. The antiparallel ordering of spins corresponding to the minimum energy of pairwise interactions cannot be realized for a triangular lattice: given the antiparallel orientation of the first and second spins on a triangle, the third spin cannot be directed strictly opposite to both the first and second ones. The minimum of the exchange energy for classical spins ($S \gg 1$) can be realized in a three-sublattice configuration in which on each triangle the spin directions make an angle of 120° with one another [1, 2]. Anderson [3]

A I Smirnov, L E Svistov, L A Prozorova P L Kapitza Institute for Physical Problems, Russian Academy of Sciences, Russian Federation
O A Petrenko University of Warwick, UK
M Hagiwara Osaka University, Japan
E-mail: prozorova@kapitza.ras.ru

Uspekhi Fizicheskikh Nauk **180** (8) 880 – 884 (2010)
DOI: 10.3367/UFNr.0180.2010081.0880
Translated by S N Gorin; edited by A Radzig

supposed that the spins $S = 1/2$ on a triangular lattice in the ground state are completely disordered and are in the state of a quantum spin liquid. Subsequent theoretical investigations based on a numerical simulation taking account of interaction between only nearest neighbors have demonstrated, however, that a three-sublattice 120° ordering arises in this case as well, but the spin reduction due to quantum zero point fluctuations is very large — the ordered spin component comes to only 40% of the nominal magnitude [4]. In experiments with real magnetic systems having a regular triangular lattice, systems with a 'triangular', i.e., three-sublattice 120° ordering, as well as quantum-disordered systems without a magnetic order, were observed as the temperature decreased to very low values (see, e.g., Ref. [5]). In this report, we consider the problem of an ordered phase of a two-dimensional antiferromagnet with quasiclassical spins on a regular triangular lattice and its phase transformations in a magnetic field.

In a magnetic field, a classical antiferromagnet with a Heisenberg exchange on a triangular lattice possesses degeneracy of a specific type [1], where all spin configurations of the three sublattices with equal total moments have the same energy in the molecular-field approximation, e.g., configurations of the a, b, b′ types in Fig. 1.

The ground state is determined in this case by fluctuations. For an equilibrium system, the free energy with allowance for quantum and thermal fluctuations, which depend on the spectra of spin waves, should be minimum. A theoretical analysis [1, 2] shows that in weak magnetic fields the fluctuations stabilize the planar spin structure (structure 'b' in Fig. 1) in which the spins lie in the plane parallel to the magnetic field. The alternative umbrella-type structure 'a' proves to be energetically unfavorable. In addition, the fluctuations stabilize a collinear spin structure of the 'two up, one down' type ('c' in Fig. 1) in a wide range of magnetic fields in the vicinity of the field equal to one third of the saturation field, $H = H_{\text{sat}}/3$. In the molecular-field approximation, such a structure can be realized only in a field $H_{\text{sat}}/3$ and does not lead to the development of any peculiarities in the magnetization curve. The allowance for fluctuations predicts the appearance of a magnetization plateau at a level of one third of the total magnetic moment and the existence of an extended (in field) region in the $T-H$ phase diagram corresponding to the collinear phase 'c'. In the region of high fields preceding the saturation field, the fluctuations stabilize the planar structure 'd'. In theoretical work and in numerical simulations (see Refs [6, 7]), the phase diagrams depicted in Fig. 2 were predicted.

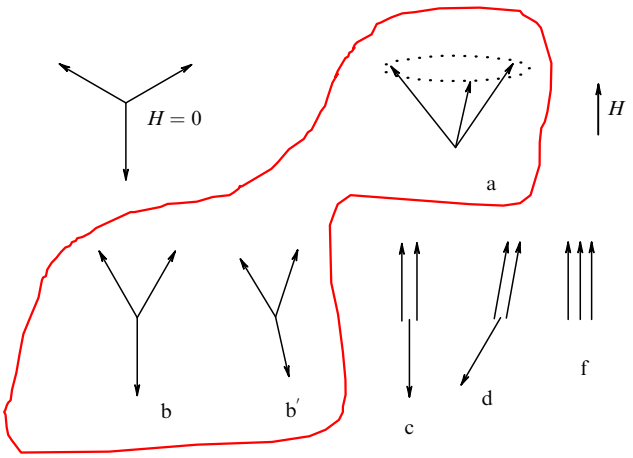

Figure 1. Schematic of magnetic moments of sublattices of a two-dimensional antiferromagnet on a triangular lattice. The outlined configurations correspond to degenerate states with the same total magnetic moment.

Among the experimental investigations of antiferromagnets on triangular lattices, studies of compounds of the ABX_3 type (A = Cs, Rb; B = Ni, Mn, Cu; X = Cl, Br, I) dominated up to recent years. However, the predominant interaction in them is exchange interaction in the direction perpendicular to planes containing triangular plane lattices of magnetic ions, i.e., these systems represent quasi-one-dimensional magnets (see, e.g., Ref. [8]). We shall consider in this report experimental investigations of a quasi-two-dimensional antiferromagnet with a triangular lattice, $RbFe(MoO_4)_2$, and compare the experimental findings with the results of theoretical models. The magnetic structure of $RbFe(MoO_4)_2$ is formed by Fe^{3+} ions ($S = 5/2$, $L = 0$) located in layers with a regular triangular (hexagonal) lattice (Fig. 3). The magnetic layers are separated by nonmagnetic Rb ions and nonmagnetic MoO_4 complexes, which substantiates the validity of the two-dimensional approximation. The moderate magnitude of the main exchange integral permits one to perform investigations in magnetic fields up to the saturation field.

In Fig. 4, the magnetization curves obtained in pulsed magnetic fields of up to 25 T are given [9], and in Fig. 5, in stationary fields up to 10 T [10]. The field was applied in the plane of magnetic layers. The data presented show the existence of a magnetization plateau near $M_{\text{sat}}/3$; as is seen from the $\mathrm{d}M/\mathrm{d}H$ curves, the plateau is expanded with

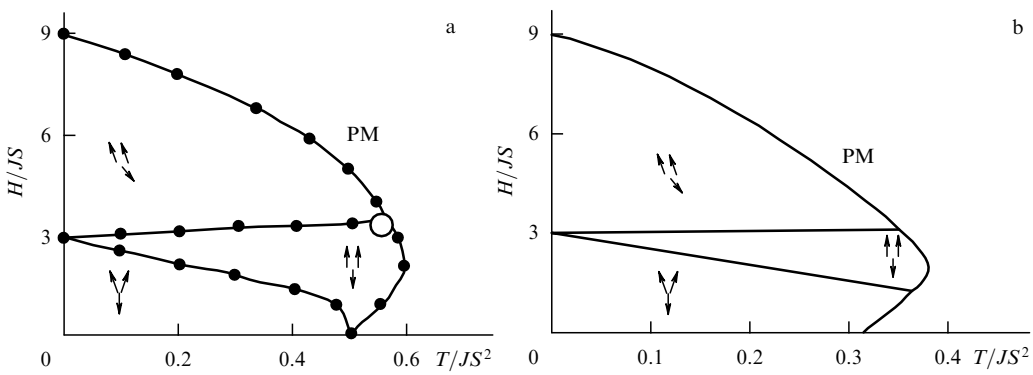

Figure 2. (a) Phase diagram for a two-dimensional XY model [6]. (b) Phase diagram for a two-dimensional Heisenberg model [7]. J is the exchange integral, S is the magnetic ion spin, and PM is the paramagnetic region.

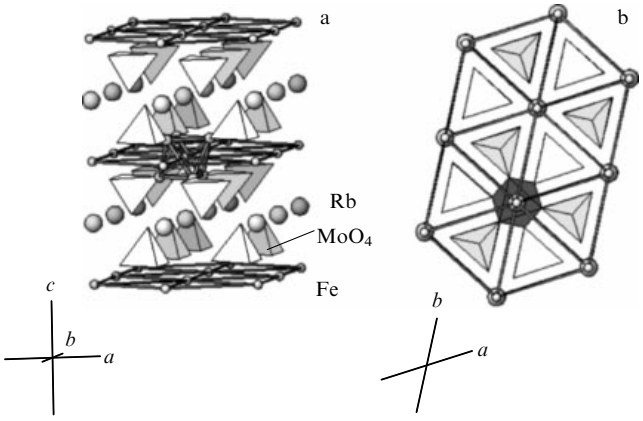

Figure 3. Crystal structure of $RbFe(MoO_4)_2$.

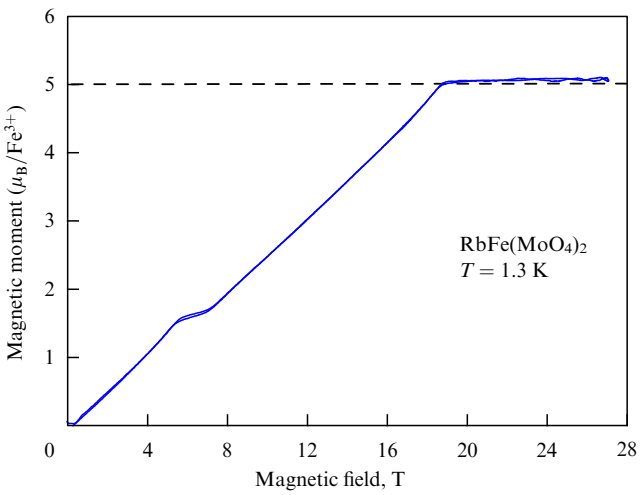

Figure 4. Field dependence of the magnetic moment in the range below 25 T.

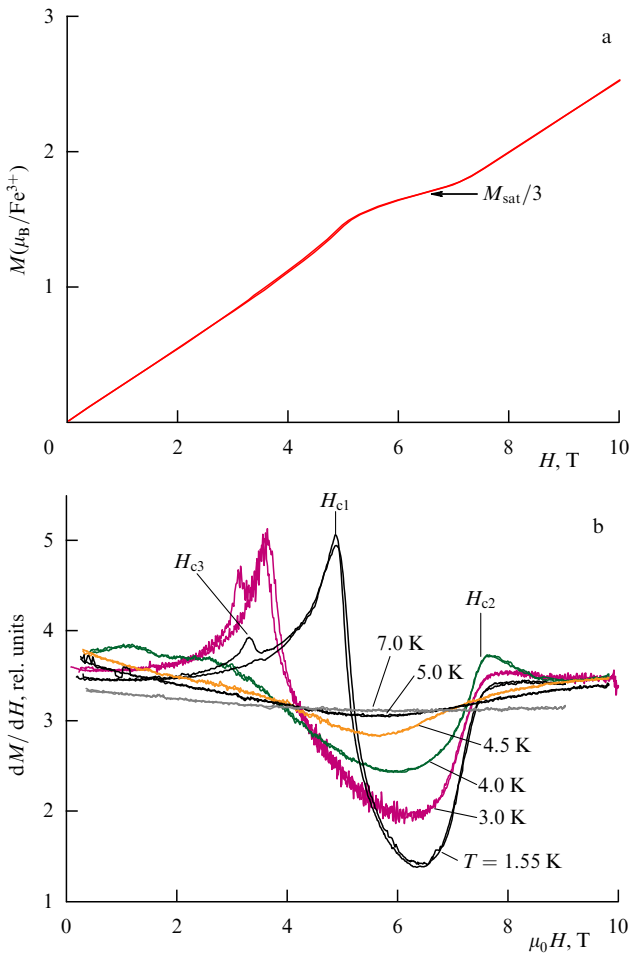

Figure 5. (a) Dependence of the magnetic moment on the field applied in the plane of magnetic layers at $T = 1.55$ K. (b) Field dependence of the derivative dM/dH at different temperatures; H_{c1}, H_{c2}, H_{c3} are the critical fields.

increasing temperature, in accordance with the fact that the thermal fluctuations stabilize the collinear phase. We shall designate the fields that bound the plateau as H_{c1} and H_{c2}. Apart from the values of these two critical fields, the variation of the derivative dM/dH reveals one more peculiarity, whose magnetic field is designated in Fig. 5 as H_{c3}; this field will be discussed below. Along with the magnetization curves, the temperature dependences of the magnetic moment in different fields [11], field and temperature dependences of the specific heat [9, 10], and spectra of electron paramagnetic resonance [9, 11] and nuclear magnetic resonance [10, 12] were also studied. The examples of the temperature dependences of the specific heat are given in Fig. 6. The data on the specific heat give clear evidence of a temperature-induced transition from the paramagnetic phase [a sharp peculiarity in the $C(T)$ curve]. When measuring $C(T)$ dependences, clear features arise in the field H_{c1} corresponding to the lower boundary of the magnetization plateau, whereas near the field of the upper boundary of the plateau the response of the heat capacity is inconspicuous. The heat capacity also exhibits a feature near the field $H_{c4} > H_{c2}$; the corresponding $C(H)$ dependences are given in Ref. [9]. All these features are presented in the phase diagram in Fig. 7.

Neutron-scattering experiments [13] reveal (in a zero field, at a temperature equal to the Néel temperature $T_N = 3.8$ K) the appearance of magnetic Bragg peaks corresponding to the wave vector $\mathbf{q} = (1/3, 1/3, 0.457)$ of the magnetic structure in the units of the reciprocal-lattice vectors of the $RbFe(MoO_4)_2$ crystal. This temperature agrees well with the temperature of the specific-heat peak and of the bend in the magnetic susceptibility curve. The values of the components (q_x, q_y) agree with the formation of a three-sublattice 120° magnetic structure in the magnetic layers of iron ions, and the value of the component q_z indicates the mutual orientation of spins in neighboring layers at an angle of 165°. Thus, the spins of magnetic ions of adjacent planes neighboring along the direction of the z-axis are ordered, deflecting from the strictly antiparallel mutual orientation, and form a spiral with an incommensurate period.

Under the action of the magnetic field applied in the plane of layers of iron ions, a change in the system of Bragg peaks occurs. In a field close to the above-mentioned H_{c3} field, a transition occurs from the incommensurate structure to a commensurate structure with a period $3c$, i.e., with a wave vector $\mathbf{q} = (1/3, 1/3, 1/3)$, and then, in greater fields exceeding the field H_{c4} which was determined when describing heat capacity, a structure with $\mathbf{q} = (1/3, 1/3, 0.41)$, incommensurate along the z-axis, is observed again. It should be noted that the low-field transition from the incommensurate to commensurate structure is likely to occur not exactly in the H_{c3} field but somewhat higher, between the fields H_{c3} and H_{c1}, since the accuracy of determining the field of transition from

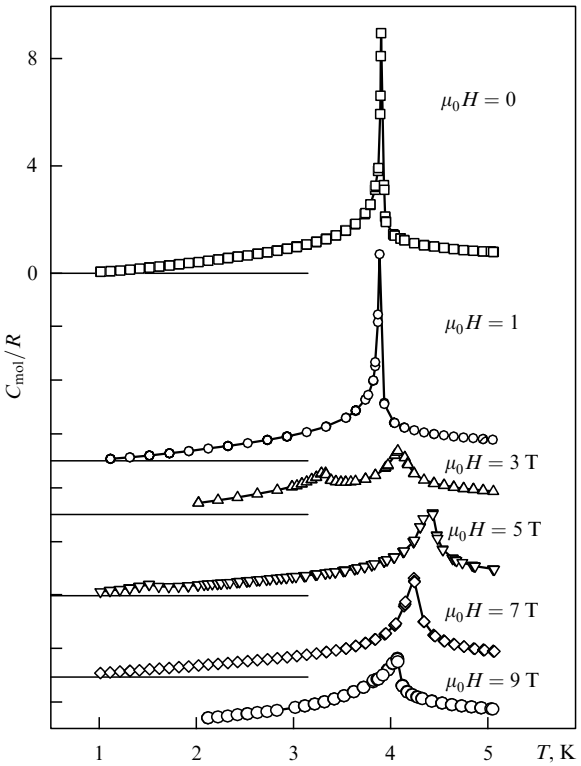

Figure 6. Temperature dependences of the heat capacity in different fields. The field is applied in the plane of magnetic layers, and R is the universal gas constant. For clarity, the curves for the nonzero values of the field are shifted downward.

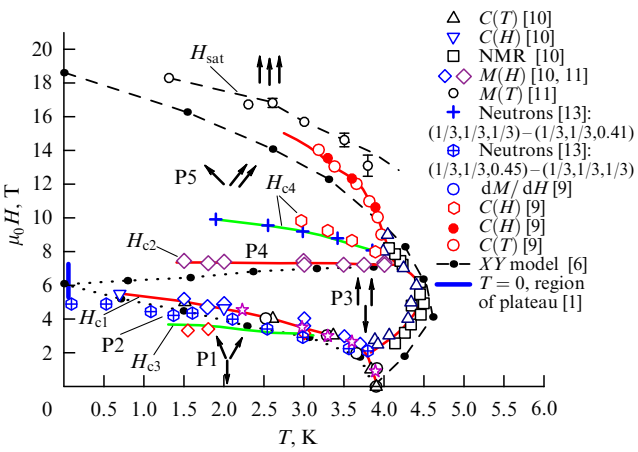

Figure 7. Phase diagram of magnetic states of $RbFe(MoO_4)_2$ for a field directed in the plane of magnetic layers: P1, P5, noncollinear incommensurate phases; P2, noncollinear commensurate three-sublattice phase; P3, collinear phase of the 'two up, one down' type (magnetization plateau), and P4, noncollinear commensurate two-sublattice phase. Arrows illustrate the spin structure of individual magnetic layers in the three-sublattice model.

one wave vector to another appears to only slightly exceed the difference $H_{c1} - H_{c3}$ (the change in the Bragg reflections arises upon a variation in the magnetic field by 1 T).

The transverse components q_x, q_y of the wave vector of the structure do not change with the variation of the magnetic field in the entire range of measurements. The changes in the structure revealed in neutron experiments are marked in the phase diagram (Fig. 7). For the high-field transition (1/3, 1/3, 1/3) $\longrightarrow$ (1/3, 1/3, 0.41), an upper boundary of the region is shown in the figure, where reflections of both types coexist. The alterations in neutron scattering related to the change in the wave vector of the structure do not fix the boundaries of the magnetization plateau (at least its upper boundary), but prove to be quite sensitive to the rearrangement of the mutual orientation of spins in the neighboring layers with respect to each other. With these rearrangements, a small-pronounced peculiarity is observed in the magnetization curve in the H_{c3} field and in the behavior of the specific heat in the H_{c4} field. The temperatures of the bifurcation of the lines of nuclear magnetic resonance (NMR) related to the appearance of an antiferromagnetic order parameter agree well with the temperatures of the specific-heat peak in the entire range of magnetic fields in which the NMR signal was detected. Thus, the different methods of investigation make it possible to determine the phase diagram of $RbFe(MoO_4)_2$ on the (T, H) plane and then to suppose that the phase transformations in fields H_{c1} and H_{c2} are connected with the phases of two-dimensional ordering in 'triangular' layers and that the rearrangement of the structure in the H_{c4} field is connected with the changes in the mutual orientation of spins in neighboring layers, being related to the three-dimensional magnetic structure. The rearrangement of the structure in the H_{c3} field appears to be also caused by changes of the latter type.

In the spectrum of electron paramagnetic resonance studied in Refs [9, 11], a splitting of magnetic resonance modes of $RbFe(MoO_4)_2$ related to the interplane exchange interaction was observed. The ratio of the exchange integrals inside a layer and between the layers that is determined from this splitting is equal to 100, i.e., $RbFe(MoO_4)_2$ is a good realization of a two-dimensional spin system. An analysis of the spectrum of electron spin resonance and the investigation of the anisotropy of the saturation field make it possible to determine the anisotropy type by two independent methods. The $RbFe(MoO_4)_2$ magnetic system has an anisotropy of the easy-plane type; the characteristic anisotropy field is $DS/g\mu_B = (5.7 \pm 0.5)$ kOe according to magnetic resonance data, and $DS/g\mu_B = (8.5 \pm 1.5)$ kOe according to data on the saturation field (here, D is the constant of uniaxial anisotropy, g is the g factor, and the corresponding spin Hamiltonian was given in Ref. [11]).

The discrepancy between the magnitudes of the characteristic anisotropy field, obtained by two different methods, which appears to be caused by the renormalization of the effective anisotropy field due to zero point fluctuations, is discussed in Refs [1, 9]. It can be expected that the behavior of a two-dimensional antiferromagnet on a triangular lattice with a strong easy-plane anisotropy will be described by the classical XY model [6]. In this case, the only parameter of the theoretical model is the exchange field JS. This quantity can be determined in an independent way from the data on the susceptibility or on the saturation field [10].

Figure 7 displays the results of such a theoretical calculation for the transition temperature from a paramagnetic phase to an ordered three-sublattice phase and for the fields H_{c1} and H_{c2} that bound the region of the magnetization plateau $M_{sat}/3$. For this construction, no adjusting parameters have been used; the magnitude of $J = 1.2$ K was taken from the observed value of the saturation field ($H_{sat} = 9JS = 182$ kOe in the notation employed in Refs [6, 7]). The theoretical value of the transition temperature $k_B T_N = 0.5JS^2$ at $S = 5/2$ and $J = 1.2$ K is in good

agreement with the observed value of 3.9 K. The boundaries between the collinear and noncollinear phases are also in satisfactory agreement with experiments. An increase in the Néel temperature under the effect of a magnetic field also corresponds to the predictions of the model. Notice that an ordinary antiferromagnet is characterized by the opposite effect of the field on the transition temperature. In the classical model [6] under consideration, the width of the interval of fields in which the fluctuations stabilize the phase with a moment $M_{\rm sat}/3$ tends to zero with decreasing temperature. The allowance for quantum fluctuations should lead to a nonzero interval at the zero temperature. The estimate of the width of this interval [1] caused by quantum fluctuations, which is shown in Fig. 7 by a vertical bar near the ordinate axis, is also in agreement with the extrapolation of the experimental dependences $H_{\rm c1}(T)$ and $H_{\rm c2}(T)$ to the zero temperature. One discrepancy with the predictions of the model is the nonzero value of the field $H_{\rm c1}$ at temperatures immediately adjoining $T_{\rm N}$ from below. It should be noted that the nonzero value of $H_{\rm c1}$ is predicted on the basis of the Heisenberg model [7]. The high-field phase boundary between the canted antiferromagnetic and paramagnetic phases also demonstrates an unordinary fluctuation behavior. In the region of temperatures exceeding 2 K, the specific-heat peak in the $C(H)$ dependence is observed in a field that is lower than the field of tending to saturation in the magnetization curve, determined from the falloff of the derivative $\mathrm{d}M/\mathrm{d}H$. The positions of the singularities in the $C(H,T)$ curves and in the $\mathrm{d}M/\mathrm{d}H$ field dependences are shown in the phase diagram in Fig. 7 near the high-field boundary of the ordered phase. The discrepancy at $T = 3$ K constitutes about 1 T. The scenario of the two-step transition to the saturated phase for a two-dimensional antiferromagnet on a triangular lattice, which was predicted in Ref. [2], is related to fluctuations: in the lower critical field, the long-range order of spin components perpendicular to the magnetic field disappears. In the interval between the two upper critical fields, the correlation between the transverse spin components falls according to a power law, with the sample remaining unsaturated. In the upper critical field, the correlations begin decreasing according to an exponential law, and the transverse component disappears.

Thus, the $RbFe(MoO_4)_2$ crystal represents a model system corresponding to a classical two-dimensional antiferromagnet on a triangular lattice. The character of the phase diagram and the existence of a magnetization plateau demonstrate good agreement with the results of a theoretical simulation of this system in terms of the classical two-dimensional XY model.

Some aspects of three-dimensional (i.e., interlayer) ordering were beyond the scope of discussion in this report; on a qualitative level they can be considered [10] based on an analysis of the interlayer interaction and related phases, which was performed in the theoretical work [14].

References

1. Chubokov A V, Golosov D I *J. Phys. Condens. Matter* **3** 69 (1991)
2. Korshunov S E *J. Phys. C* **19** 5927 (1986)
3. Anderson P W *Mater. Res. Bull.* **8** 153 (1973)
4. White S R, Chernyshev A L *Phys. Rev. Lett.* **99** 127004 (2007)
5. Nakatsuji S et al. *Science* **309** 1697 (2005)
6. Lee D H et al. *Phys. Rev. B* **33** 450 (1986)
7. Kawamura H, Miyashita S *J. Phys. Soc. Jpn.* **54** 4530 (1985)
8. Zhitomirsky M E, Petrenko O A, Prozorova L A *Phys. Rev. B* **52** 3511 (1995)
9. Smirnov A I et al. *Phys. Rev. B* **75** 134412 (2007)
10. Svistov L E et al. *Phys. Rev. B* **74** 024412 (2006)
11. Svistov L E et al. *Phys. Rev. B* **67** 094434 (2003)
12. Svistov L E et al. *Pis'ma Zh. Eksp. Teor. Fiz.* **81** 133 (2005) [*JETP Lett.* **81** 102 (2005)]
13. Kenzelmann M et al. *Phys. Rev. Lett.* **98** 267205 (2007)
14. Gekht R S, Bondarenko I N *Zh. Eksp. Teor. Fiz.* **111** 627 (1997) [*JETP* **84** 345 (1997)]

PACS numbers: 67.30.er, **75.45.+j**, **76.60.–k**
DOI: 10.3367/UFNe.0180.201008m.0884

Spin superfluidity and magnons Bose–Einstein condensation

Yu M Bunkov

The prehistory of the discovery of magnetic superfluidity goes back to the mid-1970s, when two students at Moscow Institute of Physics and Technology (MFTI in *Russ. abbr.*), Boris Dumesh and Yuriy Bunkov, started studying, under the guidance of Academician Andrei Stanislavovich Borovik-Romanov, antiferromagnetic crystals with a dynamic frequency shift. The experiments were mainly performed using $MnCO_3$ and $CsMnF_3$. In these antiferromagnets, the hyperfine field of manganese atoms gives rise to a strong polarization of ^{55}Mn nuclei, such that their frequency of precession becomes about 600 MHz. This frequency is comparable to the frequency of the low-frequency line of antiferromagnetic resonance in a weak external magnetic field. As a result, modes of coupled electron–nucleus oscillations are formed, whose frequency depends on the magnitude of interaction, viz. on the projection of the nuclear magnetic moment onto the magnetization axis of the atoms. The frequency shift of the quasi-NMR of ^{55}Mn nuclei can reach several hundred megahertz at a temperature on the order of 1 K, as is shown in Fig. 1, and decrease upon heating or upon deflection of the magnetization vector of the nuclear subsystem. This results in a strong nonlinearity of the nuclear magnetic resonance (NMR) — the frequency of the precession depends on the angle of deflection of the nuclear magnetization vector. Under these conditions, the effective mechanism of formation of a spin echo is the mechanism of frequency modulation rather than the Hahn echo mechanism. The results of successful investigations of this echo formation mechanism by the researchers of our group were reported in Refs [1–3].

The antiferromagnetic resonance can also be excited parametrically, by the modulation of the external magnetic field at a doubled frequency. It also proved possible to parametrically excite an NMR mode. A new formation mechanism of an echo was discovered, in which the echo was excited by a single resonance pulse and then by a single pulse of parametric pumping [4]. This mechanism of echo

Yu M Bunkov Institut Néel, Grenoble, France
E-mail: Yuriy.bunkov@grenoble.cnrs.fr

Uspekhi Fizicheskikh Nauk **180** (8) 884 – 889 (2010)
DOI: 10.3367/UFNr.0180.201008m.0884
Translated by S N Gorin; edited by A Radzig

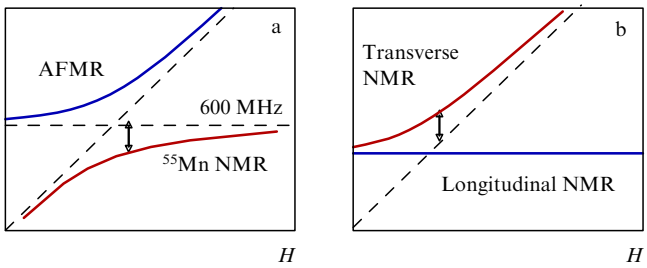

Figure 1. (a) Schematic of a spectrum of nuclear magnetic resonance (NMR) and antiferromagnetic resonance (AFMR) in $MnCO_3$. (b) Spectrum of NMR modes in superfluid ^{3}He. Arrows show the change in the NMR frequency upon nuclear magnetization deflection.

formation proved to be linear, i.e., the signal amplitude was linear in the amplitudes of both the first and second pulses [5, 6]. On the basis of the parametric mechanism of echo formation, information-processing units can be developed. All the results of our investigations into systems with a dynamic frequency shift were summed up in review paper [7].

Late in the 1970s, the superfluidity of ^{3}He was discovered, and the leading laboratories all over the world started extensive investigations of this new superfluid substance. The dynamic properties of the NMR in superfluid ^{3}He are similar to those of the systems studied in our work. A dynamic frequency shift is also observed in ^{3}He, which depends on the angle of deflection of the nuclei, as is shown schematically in Fig. 1b. Therefore, it was of interest to apply our methods of nonlinear NMR to the investigations of superfluid ^{3}He. At that time, the Institute for Physical Problems (Moscow) was fruitfully collaborating with the Low-Temperature Laboratory of the Helsinki University of Technology, where, under the guidance of Prof. Olli V Lounasmaa, investigations of superfluid ^{3}He were performed by the linear NMR methods.

Professor Lounasmaa suggested that P L Kapitza send the author of this paper to Helsinki to conduct experiments on nonlinear NMR. However, P L Kapitza and A S Borovik-Romanov decided that the idea of these investigations was so good that it was expedient to carry them out by themselves, at the Institute for Physical Problems, rather than give them up to foreign laboratories. But to conduct these studies it was necessary to construct a domestic cryostat for nuclear demagnetization and reach temperatures as low as 1 mK. To design such a cryostat, a special group was formed under the guidance of Yu M Bunkov, which included two students, V V Dmitriev and Yu M Mukharskii, and a mechanic S M Elagin.

P L Kapitza gave the green light for the fulfillment of our orders in the mechanical shop of the Institute. The construction of the cryostat for nuclear demagnetization took four years; in 1984, we obtained superfluid ^{3}He.

By that time, a number of NMR investigations of ^{3}He had been carried out at large angles of magnetization deflection, mainly at Cornell University and at Bell Laboratories, both in the United States [8]. It turned out that the induction signal in ^{3}He-A falls off quite rapidly, whereas in ^{3}He-B the longitudinal relaxation strongly depends on the magnetic field gradient, and a long-lived tail of the induction signal is observed in it. Attempts were undertaken to explain the rapid relaxation in ^{3}He-A by the magnetization transfer from the zone of sensitivity of the NMR coils by superfluid spin current, and the existence of a long-lived tail of the induction signal in ^{3}He-B, by standing spin waves. The dependence of the relaxation on the magnetic field gradient was considered at that time to be mysterious [8].

For our first experiment with superfluid ^{3}He we designed an almost closed chamber in the hope of confirming the presence of spin superfluidity in ^{3}He-A. However, the signal decayed in the closed chamber as rapidly [9] as in a chamber open at both ends, although there was no way for the magnetization to be escaped in our case! An explanation for this effect was found on the basis of the Fomin theory of the instability of homogeneous precession of magnetization in the superfluid A phase of ^{3}He [10]. Thus, the interpretation of the results of the preceding experiments as the observation of spin superfluidity in ^{3}He-A was refuted.

An unexpected result was obtained in our experiments with ^{3}He-B in the same closed chamber. We revealed that the NMR induction signal first falls off because of the inhomogeneity of the magnetic field, and then it spontaneously restores its amplitude to almost the initial magnitude [11], and that this effect is observed even at a very large inhomogeneity of the magnetic field. The results of this experiment were explained theoretically by I A Fomin as a redistribution of the magnetization deflected by the superfluid spin current [12]. In this case, a homogeneously precessing domain (HPD) is formed, in which magnetization deflected by an angle of more than 104° precesses in a spatially uniform manner. The matter is that the gradient of the precession phase creates a spin supercurrent which flows until the gradient of the precession disappears, but in ^{3}He-B this is possible only at angles of deflection exceeding 104°, at which there appears a dynamic frequency shift of a dipole–dipole nature. It is precisely this shift that compensates for the inhomogeneity of the external magnetic field. In such a way the first effect arising owing to the existence of a superfluid spin current was discovered. For this discovery, A S Borovik-Romanov, Yu M Bunkov, V V Dmitriev, Yu M Mukharskii, and I A Fomin were awarded the State Prize of the Russian Federation in 1993. A detailed analysis of the history of the discovery of spin superfluidity and its investigations can be found in Refs [13, 14].

Figure 2 displays a stroboscopic digital record of the NMR induction signal of ^{3}He in a magnetic field with strong gradient, when the inhomogeneity of the magnetic field on the scale of the chamber dimensions reaches 600 Hz. It is seen that the induction signal rapidly dephases, in approximately 2 ms. Then, a transfer of the deflected magnetization occurs in the course of 10 ms into the region of the chamber with a lower magnetic field, and an HPD is formed in the subsequent 10 ms. By applying the Holstein–Primakoff transformation, the deflected and precessing magnetization can be interpreted as the production of a gas of long-lived quasiparticles—magnons. For magnons, the gradient of a magnetic field plays the same role as a gravitational field for atoms. The field gradient and the walls of the chamber create a trap in which magnons can condense in the presence of an appropriate interaction between them. The fact that condensation occurs is seen from the spectroscopic analysis of the induction signal presented in Fig. 3. In the case of the excitation of magnons, the spectral width of the signal equals 600 Hz, which corresponds to an inhomogeneity of the magnetic field on the scale of the chamber dimensions. In 30 ms, the line collapses to a width of 0.5 Hz. This corresponds to a 1000-fold narrowing of the magnon spectrum. Such condensation had

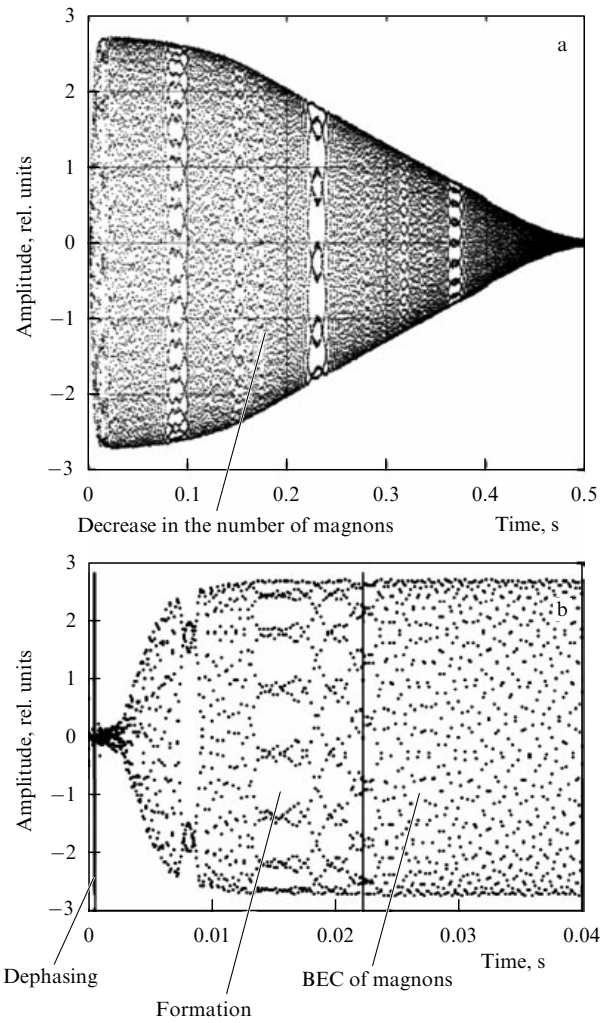

Figure 2. (a) Stroboscopic record of the induction signal. (b) The initial portion of the signal.

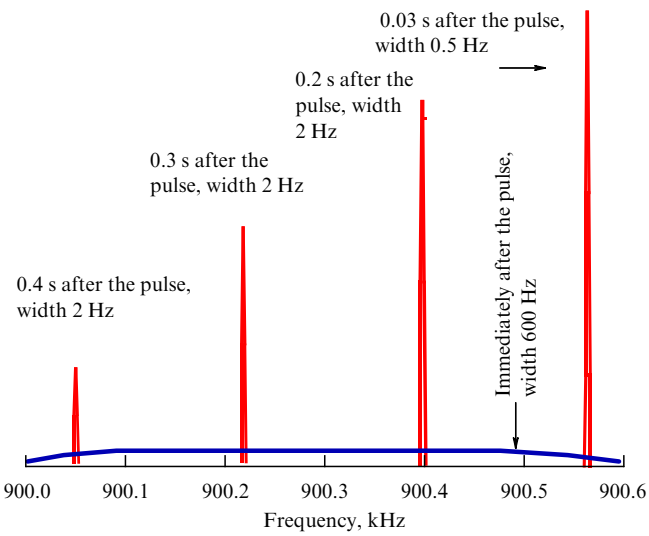

Figure 3. Spectral width of the NMR signal immediately after the arrival of a pulse and after the formation of a magnon Bose–Einstein condensate.

never been observed in an atomic Bose–Einstein condensate! A broadening of the 0.5 Hz signal arises because of the relaxation of the number of magnons.

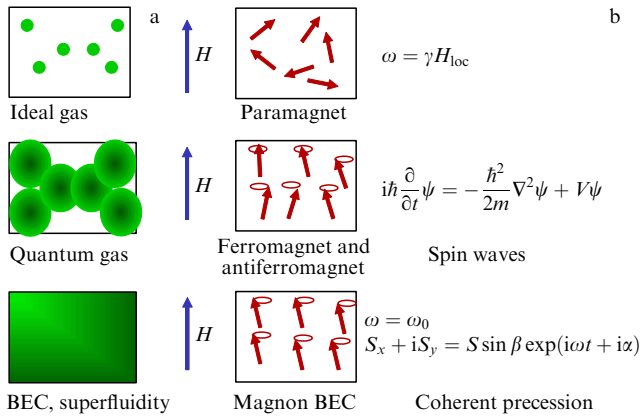

Figure 4. A schematic of the states of (a) an atomic gas, and (b) a gas of magnons: ω is the frequency of precession in a local field $H_{\rm loc}$, γ is the gyromagnetic ratio, and ω_0 is the common precession frequency.

As a result of such a weak relaxation, the signal of the Bose–Einstein condensate (BEC) is observed for a time of about 1 s. Let us recall that the atoms in the trap are also evaporated, so that the atomic BEC also lives for approximately 1 s. However, we can excite additional magnons which compensated for their natural loss; therefore, the condensate of magnons, in contrast to the atomic BEC, could exist continuously.

Figure 4 schematically depicts various states of the atomic gas and analogous states of the gas of magnons. It is necessary to distinguish the magnetically ordered state, in which spin wave modes are formed, from the state with a coherent precession, in which all magnons are described by a single wave function, just as the BEC of atoms. It is precisely the first state that was observed in experiments with a long-lived induction signal with a small amplitude [15, 16]. In these experiments, a standing spin wave was observed on the scale of the chamber sizes, whose parameters exactly corresponded to the modes of spin waves that were investigated in detail in Ref. [17]. The formation of standing spin wave modes is due to the gradient energy and boundary conditions at the walls of the chamber. In contrast, the Bose–Einstein condensation of magnons occurs due to the interaction between magnons. In this case, the NMR signal corresponds to the signal of a single oscillator whose frequency depends on the amplitude. It is this dependence that is seen well in Fig. 3. In Refs [15, 16], no dependence of the signal frequency on the amplitude was observed; therefore, these investigations cannot be considered the observation of a BEC in the form of either an HPD or a Q-ball whose properties will be considered below.

To describe the process of the Bose–Einstein condensation of magnons, we shall use the Gross–Pitaevskii equations and shall search for the solution in the form of a wave function Ψ of the homogeneous precession:

$$\Psi = \sqrt{\frac{2S}{\hbar}}\,\sin\frac{\beta}{2}\exp\left(i\omega t + i\alpha\right),$$

$$S_x + iS_y = S\sin\beta\exp\left(i\omega t + i\alpha\right),$$

which satisfy the conditions

$$\frac{\delta F}{\delta \Psi^*} = 0\,, \qquad (1)$$

$$F = \int d^3r\left(\frac{|\nabla\Psi|^2}{2m_{\rm M}} + \left(\omega_{\rm L}(z) - \omega\right)|\Psi|^2 + F_{\rm D}\right).$$

Here, S is the magnetization, S_x and S_y are its projections onto the corresponding coordinate axes, β is the angle of deflection of magnetization, and ω and α are the frequency and phase of the magnon precession, respectively.

In the last equation, the first term on the right-hand side is the gradient energy that is responsible for the formation of spin waves and superfluid spin current, and m_M is the mass of the magnon; the second term stands for the spectroscopic energy, where $\omega_L(z)$ is the Larmor frequency (the potential in the external magnetic field), ω is the magnon precession frequency (the chemical potential), and F_D is the dipole–dipole energy of interaction of the magnon with the field of magnons. For superfluid ^{3}He-B, where the orbital moment is directed along the magnetic field and the magnetization vector is deflected by an angle β, the dipole–dipole energy F_D is equal to zero for $\beta < 104°$, and to

$$F_D = \frac{8}{15}\chi\Omega_L^2\left(\frac{|\Psi|^2}{S} - \frac{5}{4}\right)^2 \qquad (2)$$

for $\beta > 104°$. Here, χ is the magnetic susceptibility, and Ω_L is the Leggett frequency characterizing the intensity of the dipole–dipole interaction. Figure 5 shows the sum of the dipole and spectroscopic energies as a function of the angle of the magnetization deflection at different values of $\Delta\omega$ — the difference between the precession frequency and the local Larmor frequency, i.e., the magnitude of the dynamic frequency shift. It is convenient to measure this shift as a percentage of the maximum possible shift, which in ^{3}He-B is equal to $\omega_d = \Omega_L^2/(2\omega_L)$. The magnons condense at a minimum energy, which arises at the angles of deflection on the order of 104°, viz. at an NMR frequency exceeding the Larmor value.

The following problem is the determination of the frequency of the nonlinear NMR. In the case of pulsed NMR, the total number of magnons produced in the experimental chamber is specified. The magnetic field gradient leads to the appearance of a gradient of the precession phase and that, in turn, gives rise to the gradient of the magnetic part of the order parameter, viz. to a superfluid magnetization transfer. This process terminates after an equilibrium distribution of magnons is reached, which corresponds to the minimum of the dipole and spectroscopic energies over the entire chamber. In this case, the system is divided into two domains. In one of them, the magnetization vector is directed along the field; in the second, a homogeneously precessing domain (HPD) arises. The dimensions of the domains are determined by the total number of magnons, and the precession frequency is determined by the Larmor frequency at the boundaries of the domains. In other words, a Bose–Einstein condensation of magnons generated by an rf pulse in the case of a pulsed NMR occurs at a minimum magnetic field. In the case of continuous NMR, the rf field specifies the frequency of the magnon precession. The equilibrium distribution of magnons corresponds to the formation of a domain with a precessing magnetization in that region of the chamber where the Larmor frequency is lower than the frequency of the rf field. In this case, the rf field specifies the chemical potential of the system, and the number of magnons is fitted to this potential. The natural relaxation of magnons in the second case is compensated for by the production of new magnons in the rf field. Thus, contrary to atomic BEC which lives in a trap for only a rather short time (on the order of 1 s), the magnon Bose–Einstein condensate can be maintained for an infinitely long time [18].

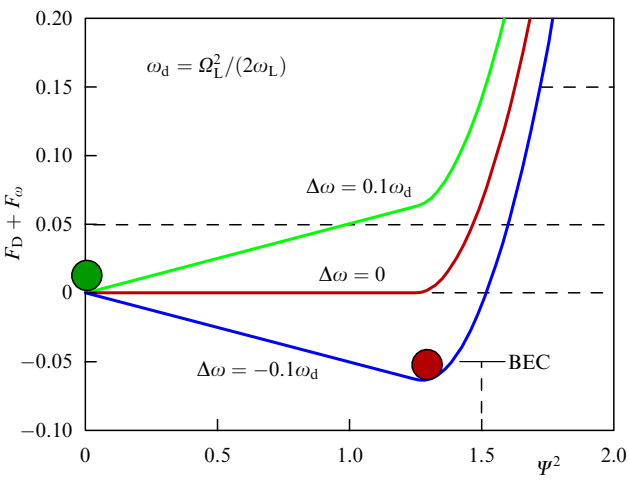

Figure 5. Spectroscopic and dipole energies as functions of the magnon density at the positive and negative difference between the NMR and Larmor frequencies. BEC arises at the minimum of the energy upon deflecting the magnetization by an angle of 104°.

This feature makes it possible to carry out a whole series of experiments with magnetic superfluidity in a channel that connects two Bose–Einstein condensates. The scheme of the experiment is demonstrated in Fig. 6. Two independent NMR spectrometers reliably shielded from one another are mounted in two chambers connected by a channel. Each spectrometer generates an HPD with a frequency and phase equal to those of the rf pumping. Condensate also fills the channel between the chambers, which we can observe with the help of miniature coils mounted in the channel. Each spectrometer measured the magnitude of the NMR signal absorption, which corresponded to the rate of magnon relaxation. When a phase difference was established between the spectrometers, a superfluid spin current began flowing through the channel, which transferred the magnetization from one chamber to another. Correspondingly, this current also transferred the Zeeman energy. As a result, the absorption signal in one chamber increased, and in the other decreased, which made it possible to measure the magnitude of the spin current. At a sufficiently high current, we managed to obtain a situation where the Zeeman energy coming into one of the chambers became so large that the absorption signal changed its sign. The BEC began emitting an rf field! Thus, we constructed a transformer based on superfluid spin current [19, 20].

Figure 6b depicts the scheme of the experimental chambers in the channel between which a constriction with an orifice diameter of 0.48 mm was arranged. The coherence length for the spin superfluidity depends on the difference between the NMR and Larmor frequencies and can reach 1 mm. By varying this difference in frequencies, we could observe a classical Josephson effect (signal *3* in Fig. 6c), a nonlinear Josephson effect (signals *2* and *4*), and a phase slippage (signal *1*) [21, 22].

Numerous other effects that confirm the magnetic coherency of the HPDs have been observed. For example, there were revealed and investigated Goldstone modes of HPDs oscillations, such as a torsional mode [23], and a surface mode [24]. A quantum vortex in a spin supercurrent was also created and studied [25]. All the results of these

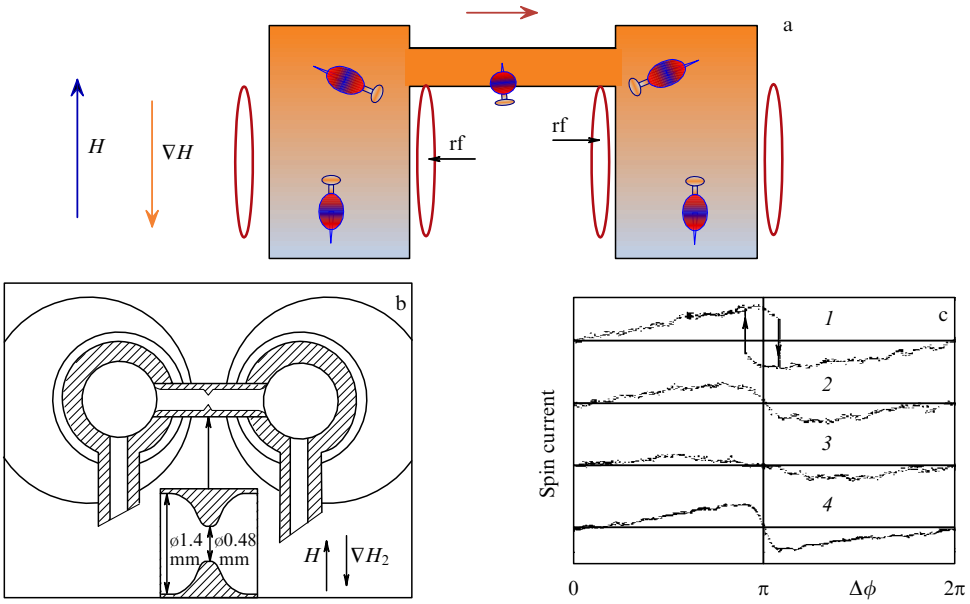

Figure 6. (a) Schematic of the experiment with two Bose–Einstein condensates connected by a channel. In the presence of a phase difference, a DC spin current flows between them; in the case of a difference in frequencies, the current increases and reaches a critical value, after which a phase slippage occurs; (b) a constriction in the channel, at which the Josephson effect was observed (c).

experiments demonstrate that an HPD is a state with a magnon Bose–Einstein condensation.

If it is assumed that only the antiferromagnetic part of the order parameter is responsible for the formation of BEC in superfluid ^{3}He, then why has the coherent state of magnons not previously been discovered in solid magnets? The reason lies in the different types of instability of the homogeneous precession and its decay into spin waves with a nonzero wave vector **k**. It turned out that in the superfluid ^{3}He as well, for temperatures $T < 0.4T_c$, where T_c is the superfluid transition temperature, an instability of the homogeneous precession also develops [26]. This instability is now explained by two mechanisms: the interaction of the precessing magnetization with the walls of the chamber [27–29], and the anisotropy of the velocity of spin waves [30]. In both cases, the instability manifests itself when, with decreasing temperature, the damping of spin waves decreases and they begin swinging parametrically. In this case, there arises a characteristic exponentially increasing curve of the decay of the homogeneous precession that was observed in Ref. [26].

In superfluid ^{3}He at lower temperatures, a new long-lived induction signal with a small amplitude was revealed, whose duration may be equal to minutes or even hours [31, 32]. After long and contradictory investigations, this signal was explained as being due to the emission of a new state of BEC produced in a trap created by the texture of the orbital part of the order parameter [33]. Here, we are dealing with the model of interaction of two quantum fields. One field, without a charge, is the field of the ^{3}He orbital moment; the other is the spin field carrying a charge. The spin field is concentrated in the minimum of the orbital field; as a result, the minimum of the orbital field decreases even greater. A situation described in the quantum theory of fields as a Q-ball arises [34]. Using very weak rf pumping, we managed to excite magnons corresponding not only to the ground state but also to excited states of the Q-ball. This was illustrated most vividly in recent experiments with a rotating cryostat for nuclear demagnetization in Helsinki, in which the profile of the orbital field was varied and, correspondingly, the frequencies of the excited states were changed [35]. After switching off the pumping, the magnons go into the ground state which emits an induction signal.

The BEC of magnons in superfluid ^{3}He is not limited to the two above-considered states. Usually, the orbital field in free ^{3}He-A is oriented transversely to the magnetic field, and the dipole–dipole energy leads to a homogeneous precession instability. In paper [36], it was predicted that the magnon BEC in ^{3}He-A can be realized if the orbital field can be aligned along the magnetic field. Recently, it was revealed that if ^{3}He-A is placed in an aerogel squeezed along the field, the anisotropy of the aerogel results in the orientation of the orbital moment along the field as well [37]. Under these conditions, a homogeneous precession [38] and the formation of BEC in ^{3}He-A [39, 40] were observed.

In addition, when the orbital moment in ^{3}He-B is oriented perpendicularly to the field, in the range of large angles of magnetization deflection a minimum of dipole energy is formed, in which the BEC can form, as was predicted in Ref. [41]. Quite recently, the formation of this BEC was revealed in Grenoble. It should be noted that all the above-mentioned types of BEC are formed not only in traps of different types but also in circumstances where various dipole–dipole interactions occur. BEC that is formed in the case of a strong counterflow of a superfluid and normal liquids in ^{3}He-B should also be mentioned [42]. Thus, to date five different states of magnon BECs in superfluid ^{3}He have been revealed. Notice also that the spin waves with a nonzero wave vector **k** can also form BEC; this was recently demonstrated in experiments with iron yttrium garnet [43]. In more detail, the properties of magnon Bose–Einstein condensates in the ^{3}He superfluid phases are considered in the reviews [44–46].

Finally, let us return to NMR in magnets with a dynamic frequency shift, which we considered at the beginning of this

paper. The dependence of the precession frequency on the angle β of deflection of the nuclear magnetization in them is described by the formula $\omega = \omega_0 - \Delta \cos\beta$. Here, ω_0 is the NMR frequency in the limit of high temperatures, and Δ is the dynamic frequency shift. Correspondingly, the energy of the hyperfine interaction varies as $F \sim -\Delta \sin\beta$, i.e., is a concave function. Consequently, under appropriate conditions BEC of magnons can occur in these magnets. In our experiments of the 1970s, a strange echo signal was observed, whose frequency corresponded to the exciting pulse frequency lying between ω_0 and $\omega_0 - \Delta$, rather than to the frequency $\omega_0 - \Delta$ of the linear NMR. We called this effect the capture echo. The capture echo is likely to have been the first observation of the magnon BEC, but this requires additional verification. At present, we are studying the Bose–Einstein condensation of magnons in solid magnets with the support of the Ministry of Education and Science of the Russian Federation (Federal Target Program 'Scientific and Pedagogical Personnel of Innovative Russia', project No. 02.740.11.5217).

Acknowledgments. In conclusion, I wish to emphasize that all our achievements are due to the support of the scientific school of the Institute for Physical Problems, RAS and to that atmosphere of confidence and benevolence which was so ably created by Andrei Stanislavovich Borovik-Romanov.

References

1. Bun'kov Yu M, Dumesh B S, Kurkin M I *Pis'ma Zh. Eksp. Teor. Fiz.* **19** 216 (1974) [*JETP Lett.* **19** 132 (1974)]
2. Bun'kov Yu M, Dumesh B S *Zh. Eksp. Teor. Fiz.* **68** 1161 (1975) [*Sov. Phys. JETP* **41** 576 (1975)]
3. Borovik-Romanov A S, Bunkov Yu M, Dumesh B S *Physica B+C* **86** 1301 (1977)
4. Bun'kov Yu M *Pis'ma Zh. Eksp. Teor. Fiz.* **23** 271 (1976) [*JETP Lett.* **23** 244 (1976)]
5. Bun'kov Yu M, Gladkov S O *Zh. Eksp. Teor. Fiz.* **71** 2181 (1977) [*Sov. Phys. JETP* **46** 1141 (1977)]
6. Bun'kov Yu M, Maksimchuk T V *Zh. Eksp. Teor. Fiz.* **79** 1408 (1980) [*Sov. Phys. JETP* **52** 711 (1980)]
7. Borovik-Romanov A S et al. *Usp. Fiz. Nauk* **142** 537 (1984) [*Sov. Phys. Usp.* **27** 235 (1984)]
8. Lee D M, Richardson R C, in *The Physics of Liquid and Solid Helium* Vol. 2 (Eds K H Bennemann, J B Ketterson) (New York: Wiley, 1978)
9. Borovik-Romanov A S, Bun'kov Yu M, Dmitriev V V, Mukharskii Yu M *Pis'ma Zh. Eksp. Teor. Fiz.* **39** 390 (1984) [*JETP Lett.* **39** 469 (1984)]
10. Fomin I A *Pis'ma Zh. Eksp. Teor. Fiz.* **39** 387 (1984) [*JETP Lett.* **39** 466 (1984)]
11. Borovik-Romanov A S, Bun'kov Yu M, Dmitriev V V, Mukharskii Yu M *Pis'ma Zh. Eksp. Teor. Fiz.* **40** 256 (1984) [*JETP Lett.* **40** 1033 (1984)]
12. Fomin I A *Pis'ma Zh. Eksp. Teor. Fiz.* **40** 260 (1984) [*JETP Lett.* **40** 1037 (1984)]
13. Bunkov Yu M, in *Low Temperature Physics* (Ed. A S Borovik-Romanov) (Moscow: MIR Publ., 1985) p. 132
14. Bunkov Yu M *Prog. Low Temp. Phys.* **14** 69 (1995)
15. Giannetta R W, Smith E N, Lee D M *J. Low Temp. Phys.* **45** 295 (1981)
16. Corruccini L R, Osheroff D D *Phys. Rev. B* **17** 126 (1978)
17. Masuhara N et al. *Phys. Rev. Lett.* **53** 1168 (1984)
18. Borovik-Romanov A S et al. *Zh. Eksp. Teor. Fiz.* **88** 2025 (1985) [*Sov. Phys. JETP* **61** 1199 (1985)]
19. Borovik-Romanov A S et al. *Pis'ma Zh. Eksp. Teor. Fiz.* **45** 98 (1987) [*JETP Lett.* **45** 124 (1987)]
20. Borovik-Romanov A S et al. *Phys. Rev. Lett.* **62** 1631 (1989)
21. Borovik-Romanov A S et al. *Pis'ma Zh. Eksp. Teor. Fiz.* **47** 400 (1988) [*JETP Lett.* **47** 478 (1988)]
22. Borovik-Romanov A S et al. *J. Physique* **49** (C-8) 2067 (1988)
23. Bun'kov Yu M, Dmitriev V V, Mukharskii Yu M *Pis'ma Zh. Eksp. Teor. Fiz.* **43** 131 (1986) [*JETP Lett.* **43** 168 (1986)]
24. Bunkov Yu M, Dmitriev V V, Mukharskiy Yu M *Physica B* **178** 196 (1992)
25. Borovik-Romanov A S et al. *Physica B* **165** 649 (1990)
26. Bunkov Yu M et al. *Europhys. Lett.* **8** 645 (1989)
27. Bunkov Yu M, Lvov V S, Volovik G E *Pis'ma Zh. Eksp. Teor. Fiz.* **83** 624 (2006) [*JETP Lett.* **83** 530 (2006)]
28. Bunkov Yu M, Lvov V S, Volovik G E *Pis'ma Zh. Eksp. Teor. Fiz.* **84** 349 (2006) [*JETP Lett.* **84** 289 (2006)]
29. Bunkov Y M, Golo V L *J. Low Temp. Phys.* **137** 625 (2004)
30. Surovtsev E V, Fomin I A *Pis'ma Zh. Eksp. Teor. Fiz.* **90** 232 (2009) [*JETP Lett.* **90** 211 (2009)]
31. Bunkov Yu M et al. *Phys. Rev. Lett.* **68** 600 (1992)
32. Bunkov Yu M et al. *Physica B* **194–196** 827 (1994)
33. Bunkov Yu M, Volovik G E *Phys. Rev. Lett.* **98** 265302 (2007)
34. Coleman S *Nucl. Phys. B* **262** 263 (1985)
35. Bunkov Yu M et al., arXiv:1002.1674
36. Bunkov Yu M, Volovik G E *Europhys. Lett.* **21** 837 (1993)
37. Kunimatsu T et al. *Pis'ma Zh. Eksp. Teor. Fiz.* **86** 244 (2007) [*JETP Lett.* **86** 216 (2007)]
38. Sato T et al. *Phys. Rev. Lett.* **101** 055301 (2008)
39. Bunkov Yu M, Volovik G E *Pis'ma Zh. Eksp. Teor. Fiz.* **89** 356 (2009) [*JETP Lett.* **89** 306 (2009)]
40. Hunger P, Bunkov Y M, Collin E, Godfrin H *J. Low Temp. Phys.* **158** 129 (2010)
41. Bun'kov Yu M, Volovik G E *Zh. Eksp. Teor. Fiz.* **103** 1619 (1993) [*JETP* **76** 794 (1993)]
42. Dmitriev V V et al. *Phys. Rev. B* **59** 165 (1999)
43. Malomed B A et al. *Phys. Rev. B* **81** 024418 (2010)
44. Volovik G E *J. Low Temp. Phys.* **153** 266 (2008)
45. Bunkov Yu M, Volovik G E *J. Phys. Condens. Matter* **22** 164210 (2010)
46. Bunkov Yu M, Volovik G E, arXiv:1003.4889

PACS numbers: 03.75.Hh, 75.30.Ds, **75.45.+j**
DOI: 10.3367/UFNe.0180.201008n.0890

Kinetics and Bose–Einstein condensation of parametrically driven magnons at room temperature

O Dzyapko, V E Demidov, S O Demokritov

The origin of the ferromagnetic state is the quantum-mechanical exchange interaction between spins of individual atoms, which aligns the spins in parallel to each other. The paramagnet–ferromagnet transition is documented by a divergence of the coherence length describing the correlation between the longitudinal components of the spins located far from each other. The fluctuations above the ground state of a ferromagnet with totally parallel spins are usually described by means of quantized low-energy spin-wave excitations, which are called magnons. Magnons in thermal equilibrium do not show coherence effects because at nonzero temperatures the transverse spin components remain uncorrelated even in a ferromagnetic phase. In fact, they are usually considered to form a gas of elementary excitations (quasi-

O Dzyapko, V E Demidov, S O Demokritov Institut für Angewandte Physik, Westfälische Wilhelms-Universität Münster, Deutschland
E-mail: demokrit@wwu.de

Uspekhi Fizicheskikh Nauk **180** (8) 890–894 (2010)
DOI: 10.3367/UFNr.0180.201008n.0890
Translated by S O Demokritov; edited by A Radzig

particles), nicely described by the quantum representation of population numbers. There have been attempts to describe coherent magnon states [1] by analogy to coherent photon states [2]. However, this description has not been well developed and has not been widely used yet for the analysis of experimental results.

Magnons are Bose particles; therefore, under particular conditions they should demonstrate Bose-Einstein condensation (BEC). However, to reach BEC at room temperature one needs to increase the chemical potential of the magnon gas above the zero value characterizing the state of true thermal equilibrium. Here we present our recent results on BEC in magnon gas driven by microwave pumping. The room-temperature kinetics and thermodynamics of magnon gas was investigated by means of the Brillouin light scattering (BLS) technique. We show that for high enough pumping powers the relaxation of the driven gas results in a quasiequilibrium state described by the Bose–Einstein statistics with a nonzero chemical potential. A further increase in the pumping power causes BEC in the magnon gas, documented by an observation of the magnon accumulation at the lowest energy level. Interference of two magnon condensates is observed as well.

One of the most striking quantum phenomena leading to spontaneous quantum coherence on a macroscopic scale is Bose–Einstein condensation. It describes the formation of a collective quantum state of bosons. As the temperature T of the boson gas decreases at a given density N or, vice versa, the number of particles increases at a given temperature, the chemical potential μ describing the gas increases as well. On the other hand, μ cannot be larger than the minimum energy of the bosons, $\varepsilon_{\min}$. The condition $\mu(N, T) = \varepsilon_{\min}$ defines a critical density $N_c(T)$. If the density of the particles in the system is larger than N_c, BEC takes place: the gas is spontaneously divided into two fractions, namely (i) incoherent particles with the density N_c distributed over the entire spectrum of possible boson states, and (ii) a coherent ensemble of particles accumulated in the lowest state with $\varepsilon = \varepsilon_{\min}$ [3].

At temperatures far below the temperature T_c of magnetic ordering, magnons can be considered as weakly interacting bosons: the Bloch law for the temperature dependence of static magnetization, which nicely describes a bulk amount of experimental data, has been obtained based on this assumption. Since magnons are bosons one can expect that they undergo the BEC transition. Several groups have reported observation of the magnetic field-induced BEC of magnetic excitations in the quantum antiferromagnets $TlCuCl_3$ [4, 5], Cs_2CuCl_4 [6, 7], and $BaCuSi_2O_6$ [8]. In these materials, a phase transition from a nonmagnetic singlet state to an ordered triplet state, accompanied by magnetic mode softening, occurs if the applied magnetic field is strong enough to overcome the antiferromagnetic exchange coupling. Such a transition can be treated as BEC in an ensemble of magnetic excitations. However, these excitations can hardly be considered as magnons — quanta of spin precession waves propagating in a magnetically ordered system.

BEC has also been observed in the ensemble of nuclear spins in superfluid ^{3}He at temperatures in the millikelvin range [9, 10]. A cell with superfluid ^{3}He was put in a strong gradient of a magnetic field. The spins were pumped by the radio-frequency radiation at the frequencies of nuclear magnetic resonance (NMR). In a pulsed NMR experiment, the magnetization of the nuclear spins was deflected by a strong pulse of the radio-frequency field, and an induction signal of the total magnetization of ^{3}He in the cell was detected by pick-up coils after the pumping pulse was switched off. Upon terminating the external pumping, the total induction signal dephased and disappeared in about 1 ms due to the strong gradient of magnetic field over the cell. However, after a transient process of about 10 ms, the induction signal corresponding to a 100% coherent precession of the deflected magnetization was detected over a long period of time up to 0.3–0.5 s. This effect is a direct manifestation of the BEC of magnons in ^{3}He.

Very recently it was shown that magnons continuously driven by microwave parametric pumping can enormously overpopulate the lowest energy level, even at room temperature [11]. This observation has been associated with the BEC of magnons. At the same time, the possibility of the BEC of quasiparticles in the thermodynamic sense is not evident [12], since quasiparticles are characterized by a finite lifetime which is often comparable to the time a system needs to reach thermal equilibrium. Moreover, an observation of the spontaneous coherence is important proof of the existence of BEC [13]. Therefore, the study of the thermalization processes for a gas of magnons and the experimental observation of the spontaneous coherence of the magnons overpopulating the lowest state are of special importance for a clear understanding of the phase transition observed in the earlier work [11].

The transition temperature of BEC in a weakly interacting gas of Bose particles with a given total density N of the particles is determined by the Einstein equation $k_B T_c = 3.31(\hbar^2/m)\, N^{2/3}$. This equation does not imply that the transition temperature should be low. Moreover, the above equation can be rewritten as $N_c^{2/3} = k_B T m/(3.31\hbar^2)$. In other words, the BEC transition can be reached at any temperature, provided the density of the particles is high enough. Below, we will demonstrate how the BEC transition can be observed at room temperature.

Experiments on the room-temperature BEC of magnons were performed on monocrystalline films of yttrium iron garnet (YIG) with a thickness of 5 μm. YIG ($Y_3Fe_2(FeO_4)_3$) is one of the most studied magnetic substances. YIG films are characterized by very small magnetic losses providing a long magnon lifetime in this substance: it appears to be much longer than the characteristic time of magnon–magnon interaction [13, 14]. This relation is a necessary precondition for Bose–Einstein condensation in a gas of quasiparticles whose number is not exactly conserved [12]. Samples with lateral sizes of several millimeters were cut from the films and were placed into a static uniform magnetic field of $H = 700-1000$ Oe oriented in the plane of the film. The injection of the magnons was performed by means of parallel parametric pumping with a frequency of 8.0–8.1 GHz. The pumping field was created using a microstrip resonator with a width of 25 μm attached to the surface of the sample. The peak pumping power was varied from 0.1 to 6 W. Details on the pumping process can be found in Refs [11, 13–15].

The redistribution of magnons over the spectrum was studied with a temporal resolution of 10 ns using time-resolved BLS spectroscopy in the quasibackward scattering geometry [16]. In this geometry, magnons from the wave vector interval $k = \pm 2 \times 10^5$ cm^{-1} determined by the wave vector of the incident light contribute to BLS spectra. Thus, the BLS intensity at a given frequency is the product of the magnon population at this frequency and the reduced density

of magnon states, taking into account the above wave vector interval alone. Giving access to the measurement of the temporal evolution of the magnon distribution, the BLS technique allows one to study the kinetics and thermodynamics of magnons. A typical frequency resolution of the experimental setup, limited by the resolution of the optical spectrometer, was 250 MHz. It was also possible to achieve a better resolution of $\Delta f = 50$ MHz, albeit at the expense of sensitivity [11]. The experiments were performed at room temperature. A detailed description of the BLS setup used can be found elsewhere [11, 13–16]

Figure 1 shows the low-frequency part of the dispersion spectrum of magnons in an in-plane magnetized ferromagnetic film, calculated for the parameters of the YIG film used and a magnetic field of $H = 700$ Oe. The solid lines represent the dispersion curves for the two limiting cases of magnons with the wave vectors **k** oriented parallel (so-called backward volume waves) or perpendicularly (so-called surface waves) to the static magnetic field **H** as indicated in Fig. 1. The both curves merge for $k = 0$ at the frequency of the uniform ferromagnetic resonance. The magnon states for intermediate angles fill the manifold between these two boundaries. As seen from Fig. 1, the manifold is characterized by a nonzero minimum frequency $f_{\min} = 2.10$ GHz corresponding to a nonzero wave vector $k_{\min} = 3 \times 10^4$ cm^{-1} aligned in parallel to the static magnetic field. The frequency minimum at a nonzero wave vector results from competition between the magnetic dipole interaction and the exchange interaction. Note that the change in the external magnetic field shifts $f_{\min}$, whereas by varying the film thickness one varies the corresponding wave vector $k_{\min}$.

Figure 1 also illustrates the process of the parametric pumping of the magnon gas. This process can be considered as the creation of two primary magnons by a microwave photon of the pumping field. It does not define the values of the magnon wave vectors. The only condition is that the two created magnons have opposite wave vectors. The pumping initiates a strongly nonequilibrium magnon distribution: a very high density of primary magnons amounting to $10^{18} - 10^{19}$ cm^{-3} is created in the phase space close to the frequency f_p. Although the primary magnons are excited by coherent pumping, they are not coherent to each other: two magnons are excited simultaneously, and only the sum of their phases, but not the phase of each magnon, is locked to the phase of the microwave pumping photon.

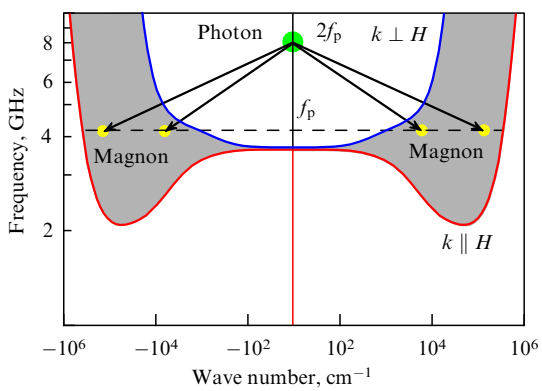

Figure 1. The low-frequency part of the dispersion spectrum of magnons in a YIG film magnetized by an in-plane static magnetic field $H = 700$ Oe. The arrows illustrate the process of parametric pumping.

Due to the intense magnon–magnon interaction, the primary magnons are rapidly redistributed over the phase space. The main mechanisms responsible for the energy redistribution *within* the magnon system are the two-magnon and the four-magnon scattering processes (see chapter 11 in book [14]). Four-magnon scattering dominates in high-quality epitaxial YIG films. It can be considered as an inelastic scattering mechanism, since it changes the energies of the scattered magnons. As a consequence, four-magnon scattering leads to the spreading of the magnons over the spectrum, keeping, however, the number of magnons in the system constant. Note here that the three-magnon scattering process which does not conserve the number of magnons does not play an important role in the described experiments [15]. In parallel, an energy transfer *out* of the magnon system due to the spin–lattice (magnon–phonon) interaction takes place. It will be shown below that the magnon–magnon scattering mechanisms preserving the number of magnons are much faster than spin–lattice relaxation. Under these conditions, a stepwise pumping should create a magnon gas characterized by a steady, quasiequilibrium distribution of magnons over the phase space after a certain transition period characterized by a thermalization time.

The magnon distributions illustrating the evolution of the magnon gas to the quasiequilibrium state are plotted in Fig. 2 for a pumping power of 0.7 W. This figure presents BLS spectra recorded for different delay times after the start of the pumping pulse. At the delay time $t = 0$, no magnons are pumped yet, and the magnon distribution corresponds to thermally excited magnons. In the early pumping stage ($t = 30$ ns), the population of magnon states close to $f_{\min}$ is not affected at all. On the contrary, the magnon density at frequencies from about 2.5 GHz to 4 GHz (the latter is close to the frequency of the primary magnons) rises significantly. Further evolution of the magnon distribution presented in Fig. 2 shows a saturation of the magnon population. In fact, the magnon population of the entire spectrum except the region close to $f_{\min}$ is saturated at $t = 60$ ns. The density of magnons close to $f_{\min}$ starts to grow for $t > 30$ ns and saturates for much larger delays, as shown in Fig. 3. The observed process can be understood as a gradual wavelike population of magnon states starting from the frequency f_p of primary magnons towards the minimum magnon frequency.

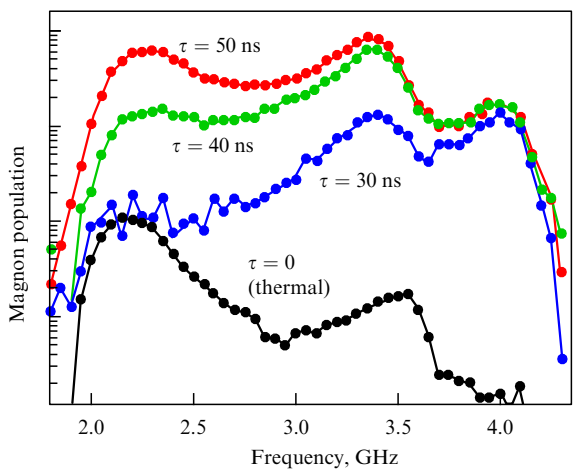

Figure 2. Evolution of the magnon population after stepwise pumping has been switched on. Note the wavelike increase in the magnon population propagating from higher frequencies toward the bottom of the spectrum.

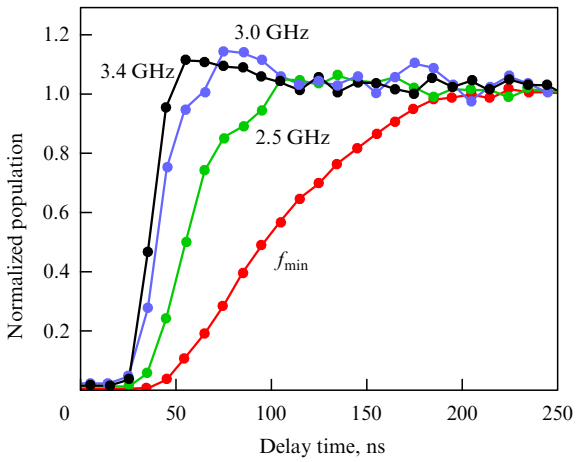

Figure 3. Evolution of the magnon population at different frequencies as a function of the delay time after stepwise pumping has been switched on. Note the slow (adiabatic) increase in the population at f_{min}.

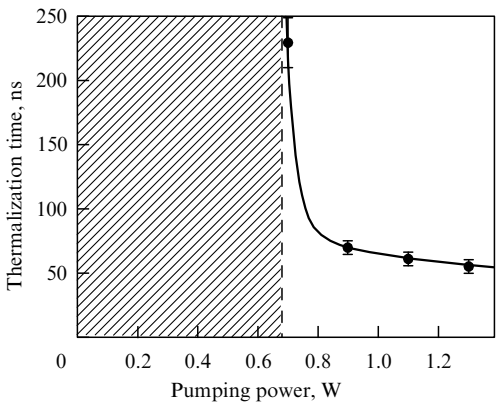

Figure 4. The magnon gas thermalization time as a function of the pumping power. The shaded area corresponds to the power below the thermalization threshold $P_{th} = 0.7$ W, where the thermalization cannot be achieved. The solid line is a guide for the eye.

This means that the increase in the population at the bottom of the spectrum takes place through multiple inelastic scattering events. Thus, a very important intermediate conclusion can be made at this point: since the magnons close to f_{min} are created through a series of multiple scattering events not conserving the phase of individual magnons, any coherence observed in the gas of magnons at the bottom of the spectrum must be a spontaneous one.

After the magnon population at the bottom of the spectrum saturates, the entire magnon gas reaches a steady state. Comparison of the measured distribution with the Bose–Einstein one confirms that this steady state corresponds to a quasiequilibrium thermodynamic state.

Due to the nonlinearity of the four-magnon scattering, the magnon thermalization time also rapidly decreases with increasing pumping power above the threshold of 0.7 W, as illustrated by Fig. 4. As seen in the figure, the thermalization time approaches a value of about 50 ns at the pumping power of 1.3 W, which is significantly lower than the lifetime of magnons in YIG films due to the spin–lattice interaction. The shaded area in the figure indicates the region of lower pumping powers, where complete thermalization of a magnon gas cannot be achieved.

After the thermal quasiequilibrium is reached, further pumping increases the density of magnons as a function of time. As a result, the value of the chemical potential μ increases as well. For the values of the pumping powers used in the experiments, this growth in μ happens much more slowly than the thermalization process; therefore, it can be considered adiabatic. Figures 5a and 5b show the measured BLS spectra at large delay times, reflecting the quasiequilibrium distributions of magnons over the phase space at different pumping powers $P = 4$ W and 5.9 W, respectively. Tokens in the figures represent the experimental data, and solid lines are the magnon distributions calculated based on the Bose–Einstein statistics [15], using μ as the fit parameter. As seen in Fig. 5a, the chemical potential grows with time, reaching saturation at $\mu/h = 2.08$ GHz. This value is close to but still below $\varepsilon_{min} = hf_{min}$. Apparently, higher values of μ

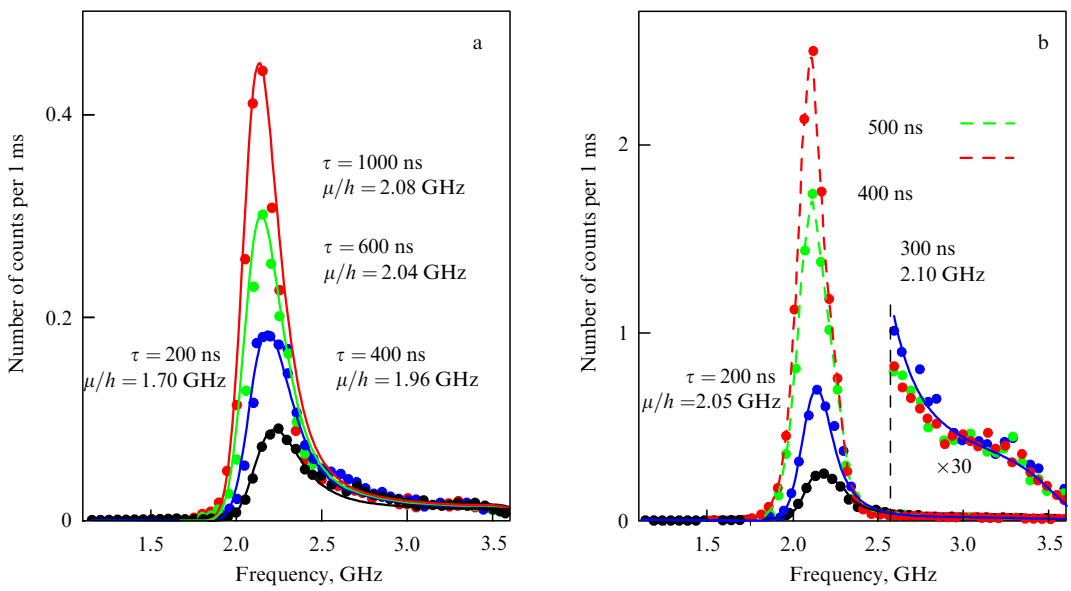

Figure 5. (a) BLS spectra from pumped magnons at a pumping power of 4 W at different delay times, as indicated. Solid lines show the results of the fit of the spectra based on the Bose–Einstein statistics, with the chemical potential being a fit parameter. Note that the critical value of the chemical potential cannot be reached at the power used. (b) Same as figure (a) for the pumping power 5.9 W. The critical value of the chemical potential is reached at 300 ns.

cannot be reached at this pumping power, since the pumped magnons leave the magnon gas due to spin–lattice relaxation. Figure 5b illustrates the processes at $P = 5.9$ W. For this pumping power, the maximum value of $\mu/h = 2.10$ GHz is reached already after 300 ns. One can conclude that the critical density N_c of the magnon gas is achieved at $t = 300$ ns, and the corresponding distribution can be considered as the critical distribution $n_c(f)$. Further pumping leads to a phenomenon which can indeed be interpreted as the BEC of magnons: all additionally pumped magnons are collected at the bottom of the spectrum without changing the population of the states with higher frequencies. This last fact is demonstrated in Fig. 5b as well, showing the high-frequency parts of the magnon distribution curves on an appropriate scale. These data demonstrate that the BLS spectra for $t > 300$ ns cannot be described just by increasing the temperature in the Bose–Einstein distribution function, since a higher temperature means higher magnon populations at *all* frequencies. Thus, Fig. 5b testifies to a formation of a Bose–Einstein condensate of magnons.

One can calculate the difference between the magnon distribution at a given time $t > 300$ ns and the critical one. One can see from Fig. 5b that this difference is nonzero just in the region close to $f_{\min}$, with the width of the region $\Delta f \approx 0.2-0.3$ GHz being defined by the resolution of the spectrometer. Optical measurements with ultimate spectral resolution have shown that the intrinsic width of the region is even below 50 MHz. Moreover, microwave spectroscopy indicates that it is narrower than 4 MHz, which corresponds to a high degree of coherence of magnons in the condensate, giving $\Delta f < 10^{-6} k_B T/h$. Thus, the narrowing of the magnon distribution with respect to that determined by the classical Boltzmann statistics is more than six orders of magnitude!

The ultimate confirmation of coherence of the observed collective quantum state might be interference of two condensates with each other. In the system studied, such an experiment can be performed in a direct way. Indeed, the magnon spectrum exhibits two degenerate minima at $k_{\min} = \pm 3 \times 10^4$ cm^{-1}; therefore, two condensates with different wave vectors are created simultaneously. The interference between them should result in a standing wave of the condensate density in real space. Figure 6a illustrates the measured profile of the condensate density. It is worth noting that, contrary to previous experiments, these measurements were not performed stroboscopically. Since each pumping pulse creates a condensate with an arbitrary phase, the phase difference between the two condensates should vary from event to event. Therefore, to detect the interference between two condensates, the pumping was applied continuously. For this purpose, a resonator allowing continuous pumping without significant overheating was designed. Thus, the values of the applied pumping powers, which allow the condensation, do not match the pumping powers corresponding to the data given in Fig. 5.

The presented profiles clearly indicate a standing wave, resulting from the interference of two condensates. To emphasize the formation of the standing wave, the Fourier transforms of the shown profiles were calculated, as illustrated in Fig. 6b. As seen from the figure, the Fourier spectra at higher pumping powers exhibit a peak whose position nicely coincides with the double value of the wave vector $k_{\min} = \pm 3 \times 10^4$ cm^{-1}. Thus, Fig. 6 undoubtedly demonstrates the coherence of the created condensates.

In conclusion, we have investigated the thermalization of a magnon gas driven by microwave parametric pumping to a quasiequilibrium state with a nonzero chemical potential. For a certain critical value of the pumping power, Bose–Einstein condensation of magnons occurs. The results obtained are in accordance with the concept of Bose–Einstein condensation and give undoubted experimental evidence of the existence of a Bose–Einstein condensate at room temperature.

Support from the Deutsche Forschungsgemeinschaft is gratefully acknowledged. S.O.D. would like to emphasize the important role of A S Borovik-Romanov in his scientific carrier.

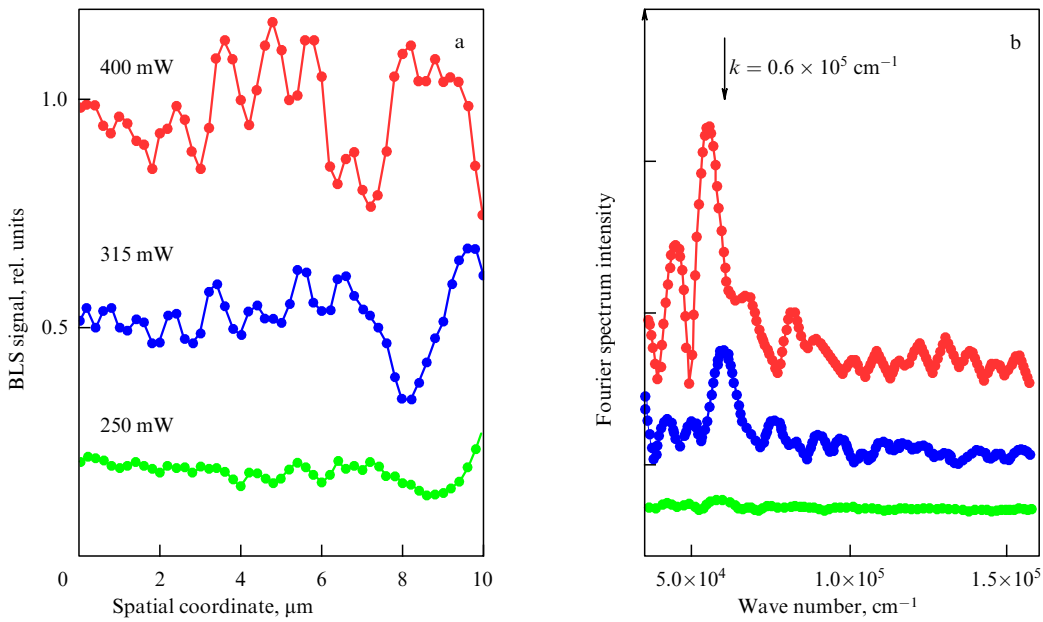

Figure 6. (a) BLS signal from two interfering condensates measured with a spatial resolution of 250 nm; (b) Fourier spectra of the spatial profiles presented in figure (a). The arrow indicates the position of the maximum calculated based on the magnon dispersion.

References

1. Rezende S M, Zagury N *Phys. Lett. A* **29** 47 (1969)
2. Glauber R J *Phys. Rev.* **131** 2766 (1963)
3. Einstein A "Quantentheorie des einatomigen idealen Gases" *Sitzungsberichte Preuβ. Akad. Wiss. Berlin* **1** 3 (1925)
4. Nikuni T et al. *Phys. Rev. Lett.* **84** 5868 (2000)
5. Rüegg Ch et at. *Nature* **423** 62 (2003)
6. Coldea R et al. *Phys. Rev. Lett.* **88** 137203 (2002)
7. Radu T et al. *Phys. Rev. Lett.* **95** 127202 (2005)
8. Jaime M et al. *Phys. Rev. Lett.* **93** 087203 (2004)
9. Bunkov Yu M, Volovik G E *J. Low Temp. Phys.* **150** 135 (2008)
10. Volovik G E *J. Low Temp. Phys.* **153** 266 (2008)
11. Demokritov S O et al. *Nature* **443** 430 (2006)
12. Snoke D *Nature* **443** 403 (2006)
13. Demidov V E et al. *Phys. Rev. Lett.* **100** 8047205 (2008)
14. Demidov V E et al. *Phys. Rev. Lett.* **99** 037205 (2007)
15. Dzyapko O et al. *New J. Phys.* **9** 64 (2007)
16. Demokritov S O, Hillebrands B, Slavin A N *Phys. Rep.* **348** 441 (2001)
17. Sparks M *Ferromagnetic-Relaxation Theory* (New York: McGraw-Hill, 1964)